Dispersion in Radial Flow from a Recharge Well

JOHN A. HOOPES

Department of Civil Engineering, University of Wisconsin
Madison, Wisconsin 53706

DONALD R. F. HARLEMAN

Department of Civil Engineering, Massachusetts Institute of Technology
Cambridge, Massachusetts 02139

The recharge and disposal of treated and untreated waste waters in groundwater aquifers results in a mixing of these waters with the natural groundwater. The distribution and boundaries of the ensuing mixture are determined by the combined mechanisms of convection, dispersion, diffusion, and sorption. In this study, the mass conservation equation for a dissolved substance in two-dimensional groundwater flow is developed. An analytical solution and a numerical solution of this equation are obtained for the radial and temporal distribution of a conservative, dissolved substance, which is injected into a homogeneous isotropic confined aquifer by a single recharging well. Experimental measurements of the concentration distributions of a dilute salt water tracer support the theoretical solutions. It is found that, for homogeneous media, the dispersed or mixed region may be less than 1% of the volume of fluid recharged at distances of only 30–60 meters from the well. Finally, from the experimental results it is shown that the dispersion coefficient along the streamlines is the same for both uniform and nonuniform flows at the same velocity.

INTRODUCTION

The successful operation of a recharge or disposal well requires a knowledge of how the recharged water or wastes will be distributed throughout a groundwater basin and what effects there will be on the quality of the natural groundwater. The resulting water quality is a complex problem requiring an understanding of the effects of adsorption, decay, aeration, and dilution by mixing on the chemical, biological, and radiological constituents in the water moving through the soil. The movements and distribution of waters within a groundwater basin are studied by means of tracers and observation wells. The interpretation of such studies, however, requires a knowledge of the mechanics of miscible fluid displacement since tracers, like recharged waters and wastes, are miscible with the natural groundwater.

Studies on longitudinal and lateral dispersion in flow through porous media date from *Kitagawa's* [1934] work; however, during the last 10 to 15 years, numerous investigators (see summaries of this work in *Harleman and Rumer* [1962] and *Hoopes and Harleman* [1965]) have presented theoretical models and experimental measurements of this phenomenon. These theoretical descriptions of dispersion have employed either a statistical analysis of the fluid particle motion through a porous media or a mass conservation requirement on a tracer traveling with the fluid.

The earliest studies on dispersion in well recharge were reported by the *Sanitary Engineering Research Laboratory* [1955]; this work involved a field study using both fresh and treated waste water. Bacteria in the waste water were adsorbed by the media within 100 feet of the well, independent of recharge rate or period of recharging; however, chemical constituents in the water were not attenuated but were transported with the recharged water. This study was followed with some laboratory model tests and some additional field testing of different tracers by *Lau et al.* [1957]. *Ogata* [1958] obtained an integral solution to the radial flow-dispersion equation; however, the solution was not evaluated. *Lau et al.* [1959] reported on an approximate expression for the spread (standard deviation) of a tracer distribution in radial flow; laboratory model

studies supported their derived expression. *Raimondi et al.* [1959] modified the dispersion term in the tracer conservation equation and obtained a solution for the tracer distribution in radial flow due to a slug injection at the recharge well. *Harpaz and Bear* [1964] presented some results of laboratory and field tests on underground storage operations with a single recharging well. No solution was given for the tracer distribution including dispersion; estimates of the longitudinal dispersion coefficient were made, using the results of *Lau et al.* [1959].

In this paper, the mass conservation equation for a dissolved substance in two-dimensional groundwater flow is developed. In the case of radial flow from a well, a simple, approximate expression for the radial and temporal distribution of a dissolved substance introduced at the well is obtained. A comparison of the approximate expression with a numerical solution to the differential equation is given in order to define the region in which the approximate solution is valid. In addition, some measured tracer distributions in a laboratory model are presented to verify the theoretical predictions and to show the relative importance of convection, dispersion, and diffusion on the displacement process in a laboratory model and a field situation.

Notation

A, $Q/2\pi b\theta$, cm²/sec.
b, thickness of confined aquifer, cm.
c, concentration of tracer, mass of tracer/mass of solution.
c_0, tracer concentration at point of tracer injection.
d_{50}, mean particle size of porous medium, cm.
D_1, coefficient of longitudinal dispersion in uniform flow, cm²/sec.
D_1', D_2', coefficients of longitudinal and lateral dispersion in nonuniform flow, cm²/sec.
D_m, molecular diffusion coefficient, cm²/sec.
G, dimensionless concentration ratio, c/c_0.
h, piezometric head, cm.
k, integer, 0, 1, 2, 3.
K, Darcy permeability, cm/sec.
m, integer, 0, 1, 2, 3.
n, coordinate along an equipotential line, cm.
n_1, exponent on the velocity in the longitudinal dispersion coefficient.
q, seepage velocity along a streamline, cm/sec.
r, ω, z, cylindrical coordinates, cm.
r_w, radius of a well, cm.
$\mathcal{R}$, Reynolds number $= qd_{50}/\nu$.
s, coordinate along a streamline, cm.
S, rate of gain of tracer in the control volume, mass/sec.
t, time, sec.
t_{50}, time at which $c/c_0 = \frac{1}{2}$ any point, sec.
t_{50_r}, time at which $c/c_0 = \frac{1}{2}$ in recharge well, sec.
t_*, $t - t_{50_r}$, sec.
UC, uniformity coefficient of particle size distribution $= d_{60}/d_{10}$.
α_1, longitudinal dispersivity coefficient in uniform flow, cm.
α_1', α_2', longitudinal and lateral dispersivity coefficient in nonuniform flow, cm.
η, $(8/3)(\alpha_1'/r)$.
θ, porosity.
μ, $3D_m r/4\alpha_1' A$.
ν, kinematic viscosity, cm²/sec.
ξ, $2At_*/r^2$.
$\bar{\rho}$, solution density, mass of solution/volume of solution.
ρ, dimensionless radial coordinate, r/α_1'.
σ, standard deviation of concentration distribution, cm.
τ, dimensionless time coordinate $= At/\alpha_1'^2$.
ϕ, equipotential function, cm²/sec.
ψ, stream function, cm²/sec.
ψ_1, coefficient of dispersion coefficient correlation with Reynolds number.
$\mathrm{erf}_c(\Delta)$, complementary error function of

$$\Delta = \frac{2}{\sqrt{\pi}} \int_{\Delta}^{\infty} e^{-\lambda^2}\, d\lambda$$

Analytical Framework

Convective-dispersion equation for two-dimensional flows. A substance (i.e., tracer or pollutant material) introduced into a flow, over an area or at a point, will be moved away from its point of introduction and distributed throughout the flow by the combined mechanisms of convection, dispersion, diffusion, and sorption. For any flow, the resulting time and spatial distribution of a substance can be obtained from

the condition that the substance must be conserved.

Consider a two-dimensional laminar flow through a porous medium with part of its streamline and equipotential pattern as shown in Figure 1. In Figure 1, q_1 and q_2 are the average seepage velocities in the two stream tubes, and ΔQ is the discharge in each stream tube. Darcy's law is assumed to govern the flow; hence, the flow satisfies Laplace's equation ($\nabla^2\phi = 0$ and $\nabla^2\psi = 0$), where lines of constant ϕ and ψ form an orthogonal, curvilinear coordinate system. s and n are orthogonal coordinates along the streamlines and equipotential lines, respectively.

For a small volume of the flow field $\Delta n \Delta s \Delta z$ (Δz is the thickness of the small volume perpendicular to the plane of flow), the mass conservation requirement for a substance introduced into the flow is expressed by the equation (see *Hoopes and Harleman* [1965])

$$\frac{\partial}{\partial t}(\bar{\rho}c\ \Delta s\ \Delta n\ \Delta z\ \theta) + \frac{\partial}{\partial s}(\bar{\rho}cq\ \Delta n\ \Delta z\ \theta)\ \Delta s = \frac{\partial}{\partial s}\left[(D_1' + D_m)\frac{\partial}{\partial s}(\bar{\rho}c)\ \Delta n\ \Delta z\ \theta\right]\Delta s + \frac{\partial}{\partial n}\left[(D_2' + D_m)\frac{\partial}{\partial n}(\bar{\rho}c)\ \Delta s\ \Delta z\ \theta\right]\Delta n + S \tag{1}$$

In equation 1, $\bar{\rho}$ is the average solution density (mass of solution/volume of solution), c is the average concentration of substance (mass of substance/mass of solution), θ is porosity, D_1', D_2', and D_m are coefficients of longitudinal and lateral dispersion and molecular diffusion, respectively, and S is the rate of gain of substance within the volume due to leaching from the porous material or chemical reaction. It has been assumed in the development of equation 1 that there is no mass flux in the z direction (i.e., $\partial c/\partial z = 0$). The two terms on the left side of equation 1 represent the time rate of change of substance within the pore volume $\Delta s \Delta n \Delta z \theta$ and the net rate of efflux of substance from this volume by convection with the average seepage velocity q. The first two terms on the right side of equation 1 express the net rate of efflux of substance from the pore volume by dispersion and molecular diffusion. The dispersion coefficients, D_1' and D_2', result from variations of the seepage velocity from the mean seepage velocity in the pore volume [*Rumer*, 1962; *Scheidegger*, 1961]; models of their dependence on pore geometry and seepage velocity have seen discussed by *Scheidegger* [1961] and *Bear* [1961].

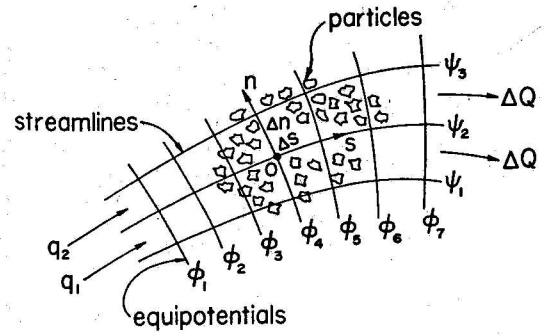

Fig. 1. Streamline and equipotential pattern for a steady two-dimensional flow.

In this paper, the substance is assumed to be conservative, and the density variations due to the substance are negligible. Thus, S is equal to zero and $\bar{\rho}$ is equal to a constant. Experimental evidence [see *Harleman and Rumer*, 1962; *Hoopes and Harleman*, 1965] indicates that the dispersion coefficients for uniform flow vary with the seepage velocity to a power different from 1; however, if the seepage velocity variations throughout the flow field are not large (i.e., variations less than about one order of magnitude), the dispersion coefficients vary nearly linearly with the seepage velocity. For nonuniform flows, it will be assumed that the dispersion coefficients vary linearly with the seepage velocity and are given by

$$D_1' = \alpha_1' q \tag{2}$$

$$D_2' = \alpha_2' q \tag{3}$$

α_1' and α_2' are constants, called intrinsic dispersivity coefficients, that are functions of the media structure only.

Introducing these assumptions into equation 1 allows it to be simplified to

$$\frac{\partial c}{\partial t}\Delta s\ \Delta n + \frac{\partial}{\partial s}(cq\ \Delta n)\ \Delta s = \frac{\partial}{\partial s}\left([\alpha_1' q + D_m]\frac{\partial c}{\partial s}\Delta n\right)\Delta s + \frac{\partial}{\partial n}\left([\alpha_2' q + D_m]\frac{\partial c}{\partial n}\Delta s\right)\Delta n \tag{4}$$

Since the streamline and equipotential line

pattern approximates squares in the x-y plane, $\Delta s \cong \Delta n$ (see Figure 1). In addition, as $q\Delta n =$ flow through a stream tube, we have

$$-\Delta\psi = \Delta Q = q\,\Delta n \cong q\,\Delta s = \text{constant} \quad (5)$$

for all stream tubes, independent of Δs or Δn. Using equation 5 in equation 4, with the approximately equal sign replaced by an equal sign, gives

$$\frac{\partial c}{\partial t} + q\frac{\partial c}{\partial s} = [\alpha_1' q + D_m]\frac{\partial^2 c}{\partial s^2} + [\alpha_2' q + D_m] \cdot \frac{\partial^2 c}{\partial n^2} + \frac{D_m}{\Delta n}\frac{\partial c}{\partial s}\frac{\partial(\Delta n)}{\partial s} + \frac{D_m}{\Delta s}\frac{\partial c}{\partial n}\frac{\partial(\Delta s)}{\partial n} \quad (6)$$

where D_m has been assumed constant. In this form equation 6 is the general convective-dispersion equation for a conservative tracer dispersing in a plane, laminar flow through a porous medium, with s and n as coordinates along the streamlines and equipotential lines, respectively.

Equation 6 can also be expressed in terms of the stream function and equipotential function, ψ and ϕ. Since

$$q = d\phi/ds = d\psi/dn \quad (7)$$

and

$$d\psi/ds = d\phi/dn = 0 \quad (8)$$

$$\frac{\partial}{\partial s} = \frac{\partial}{\partial \phi}\cdot\frac{d\phi}{ds} = q\frac{\partial}{\partial \phi} \quad (9)$$

and

$$\frac{\partial}{\partial n} = \frac{\partial}{\partial \psi}\cdot\frac{d\psi}{dn} = q\frac{\partial}{\partial \psi} \quad (10)$$

Using equations 7, 9, and 10, equation 6 can be written

$$\frac{\partial c}{\partial t} + q^2\frac{\partial c}{\partial \phi} = q^2\frac{\partial}{\partial \phi}\left([\alpha_1' q + D_m]\frac{\partial c}{\partial \phi}\right) + q^2\frac{\partial}{\partial \psi}\left([\alpha_1' q + D_m]\frac{\partial c}{\partial \psi}\right) \quad (11)$$

Equation 11 is another useful form of the general convective-dispersion equation for two-dimensional laminar flows. For $D_m = 0$, *Bachmat and Bear* [1964] have also obtained equations 6 and 11. They arrived at these equations, however, by first expressing the conservation of mass equation in a general tensorial form, suitable for any coordinate system; in the case of plane flows, their results reduce to equations 6 and 11.

Dispersion in steady, radial flow from a line source. The flow field in this study is generated by a vertical line source, along the z axis at $r = 0$, which discharges fluid at a constant rate Q into a homogeneous, isotropic aquifer of infinite, horizontal extent. The aquifer is confined by two parallel planes, perpendicular to the z axis and spaced a distance, b, apart (see Figure 2).

The seepage velocity at any radius, obtained from the continuity equation, is

$$q = \frac{Q}{2\pi b r\theta} = \frac{A}{r} \quad (12)$$

where θ = porosity and $A = Q/2\pi b\theta$. Away from the immediate vicinity of the source, the flow will be laminar and governed by Darcy's law, $q = -(K/\theta)\ (\partial h/\partial r)$, where K is the permeability of the media, h is the piezometric head at any radius r. Combining Darcy's law with equation 12 and integrating gives

$$h_1 - h_2 = \frac{Q}{2\pi bk}\ln\frac{r_2}{r_1} \quad (13)$$

for the head distribution in the aquifer. h_1 and h_2 are the piezometric heads at r_1 and r_2.

The general equation describing the spatial and temporal distribution of a dissolved substance introduced at the line source (or any other point) is given by equations 6 or 11. In terms of the r and ω coordinates, equation 6 becomes

$$\frac{\partial c}{\partial t} + \frac{A}{r}\frac{\partial c}{\partial r} = \alpha_1'\frac{A}{r}\frac{\partial^2 c}{\partial r^2} + \alpha_2'\frac{A}{r}\frac{\partial^2 c}{r^2\,\partial\omega^2} + \frac{D_m}{r}\frac{\partial}{\partial r}\left(r\frac{\partial c}{\partial r}\right) + D_m\frac{1}{r^2}\frac{\partial^2 c}{\partial\omega^2} \quad (14)$$

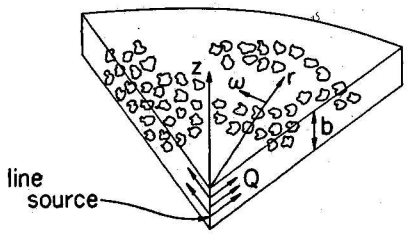

Fig. 2. Flow field and coordinate system for dispersion in radial flow from a line source.

with $s = r$, $n = r\omega$, $\Delta s = \Delta r$, $\Delta n = r\Delta\omega$, and $q = A/r$. If we assume that the concentration distribution is symmetrical with respect to ω, equation 14 reduces to

$$\frac{\partial c}{\partial t} + \frac{A}{r}\frac{\partial c}{\partial r} = \alpha_1' \frac{A}{r}\frac{\partial^2 c}{\partial r^2} + \frac{D_m}{r}\frac{\partial}{\partial r}\left(r\frac{\partial c}{\partial r}\right) \quad (15)$$

Ogata [1958] has obtained a solution to equation 15 in integral form for the case where $D_m = 0$ and a substance is introduced when $t = 0$ at $r = r_w$ (r_w is the well radius) and the concentration of tracer at $r = r_w$ is maintained constant for $t > 0$. This integral solution is too complicated to evaluate analytically, even for the case of $r_w = 0$ (i.e., a line source), and a numerical integration of the integral would be required. In lieu of a numerical integration of *Ogata's* [1958] solution, a direct numerical solution of equation 15 and several other analytical approaches to solving equation 15 with $D_m = 0$ were tried.

For $D_m = 0$, equation 15 was solved by using an explicit numerical technique on an IBM 7094 computer. To generalize the results of the numerical solution, equation 15 was first expressed in dimensionless form as

$$\frac{\partial G}{\partial \tau} + \frac{1}{\rho}\frac{\partial G}{\partial \rho} = \frac{1}{\rho}\frac{\partial^2 G}{\partial \rho^2} \quad (16)$$

where $G = c/c_0$, $\rho = r/\alpha_1'$, $\tau = At/\alpha_1'^2$ and c_0 is the concentration of tracer at the point $r = 0$. To carry out a numerical solution of equation 16, the continuous (ρ, τ) plane is replaced by a grid or mesh of points, spaced $\Delta\rho$ and $\Delta\tau$ apart, such that $\rho = k\Delta\rho$ and $\tau = m\Delta\tau$, where k and m are the integers 1, 2, 3, $\cdots$ and $\Delta\rho$ and $\Delta\tau$ are constant. In addition, the continuous derivatives in equation 16 are replaced by finite approximations, derived from Taylor series expansions of the relative concentration G about each mesh point (ρ, τ). With these approximations, equation 16 can be expressed in finite difference form as (for details see *Hoopes and Harleman* [1965])

$$G_{k,m+1} = G_{k,m}\left(1 - \frac{2\,\Delta\tau}{k(\Delta\rho)^3}\right) + G_{k+1,m}\left(\frac{\Delta\tau}{k(\Delta\rho)^3} - \frac{\Delta\tau}{2k(\Delta\rho)^2}\right) + G_{k-1,m}\left(\frac{\Delta\tau}{k(\Delta\rho)^3} + \frac{\Delta\tau}{2k(\Delta\rho)^2}\right) \quad (17)$$

in which $G_{k,m}$ is the relative concentration at the point $\rho = k\Delta\rho$ at time $\tau = m\Delta\tau$. Thus, knowing the values of G at all the spatial mesh points k, for one time m, the time history of relative tracer concentration G can be determined at each spatial mesh point k by using equation 17. The boundary and initial conditions applied in the computations were $G(k = 0, m = 0) = \frac{1}{2}$, $G(k = 0, m \geq 1) = 1$, and $G(k \geq 1, m = 0) = 0$. These initial and boundary conditions correspond to a step function being introduced at $\rho = 0$ and $\tau = 0$, where the value of G at $\rho = \tau = 0$ was set equal to $\frac{1}{2}$ because of the concentration discontinuity. In order for equation 17 to predict the tracer concentration distribution described by equation 16, the mesh size $\Delta\rho$ and $\Delta\tau$ must be chosen in such a way that equation 17 will be stable and converge to the exact solution of equation 16. Stability of the difference equation 17 requires that $G_{k,m+1}$ be bounded; thus, equation 17 will be stable provided that the coefficients of each of the terms on the right-hand side of equation 17 are positive and their sum is equal to 1 and the initial distribution, $G_{k,0}$ is bounded [see *Richtmyer*, 1962, p. 13]. Convergence of equation 17 to the exact solution of equation 16 follows from the stability criteria, using Lax's equivalence theorem [see *Richtmyer*, 1962, pp. 14, 15, and 44]. Thus, for stability and convergence

$$1 - 2\,\Delta\tau/k(\Delta\rho)^3 \geq 0 \quad (18)$$

and

$$\frac{\Delta\tau}{k(\Delta\rho)^2}\left(\frac{1}{\Delta\rho} - \frac{1}{2}\right) \geq 0 \quad (19)$$

For these conditions to hold,

$$\Delta\rho \leq 2 \quad (20)$$

and

$$\Delta\tau \leq (\Delta\rho)^3/2 \leq 4 \quad (21)$$

since the critical case occurs when $k = 1$ ($G = 1.0$ for $k = 0$).

To test the influence of mesh size $\Delta\rho$ and $\Delta\tau$ on the rate of convergence of equation 17 to equation 16 two numerical solutions of equation 17 were carried out; in the first case, $\Delta\rho = 1$, $\Delta\tau = \frac{1}{4}$ and in the second case, $\Delta\rho = 2$, $\Delta\tau = 4$. The results for the numerical solu-

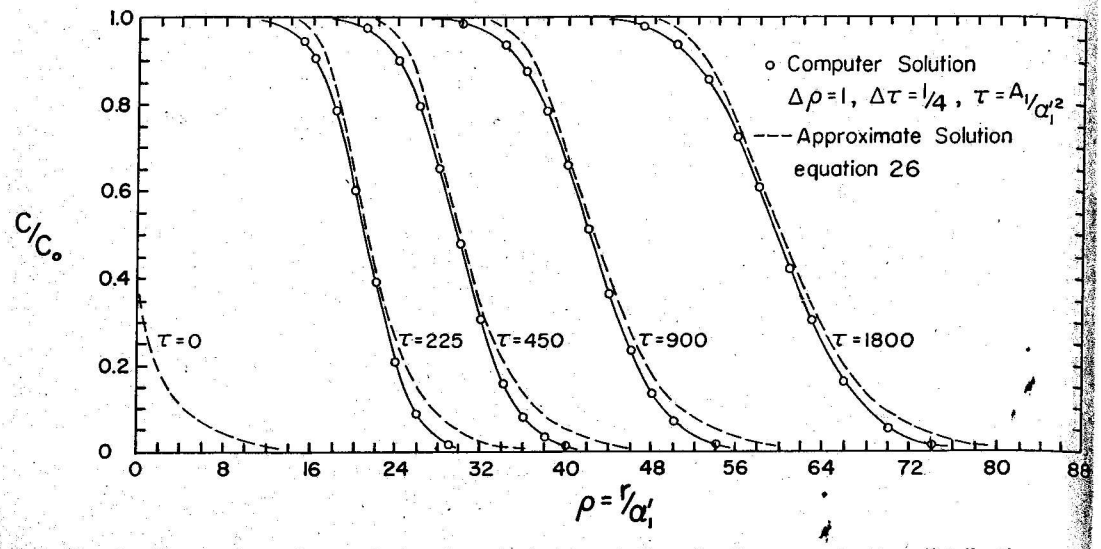

Fig. 3. Comparison of numerical and approximate solutions for the concentration distribution in radial flow.

tion for G in the first case are plotted in Figure 3 for $\tau = 0$, 225, 450, 900, and 1800. For the second case, the numerical solution is plotted in Figure 4 for $\tau = 1856$ and 8040. In addition, the numerical solution at $\tau = 1856$ with $\Delta\rho = 1$ and $\Delta\tau = 1/4$ is also plotted in Figure 4. Comparing the numerical solutions for the two mesh sizes at $\tau = 1856$ shows that the concentration distributions are in close agreement; hence, for $\tau > 2000$, the coarser mesh size will

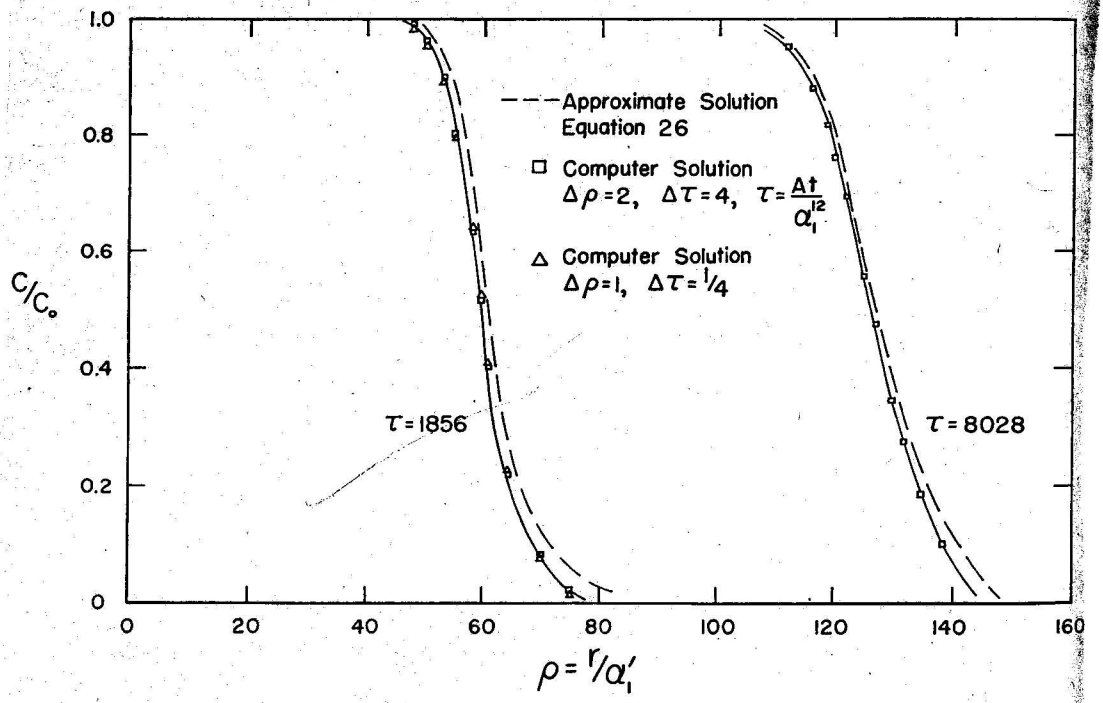

Fig. 4. Comparison of numerical and approximate solutions for the concentration distribution in radial flow.

give a good approximation to the exact solution of equation 16. For very small values of ρ, a mesh smaller than $\Delta\rho = 1$ and $\Delta\tau = \frac{1}{4}$ should be used; however, as the errors in the concentrations introduced at any τ by the mesh size will be damped within a few time steps (since the numerical solution is stable), and since the concentration distributions very close to the source ($\rho = 0$) were not needed in the experimental work, no calculations with a finer mesh size were performed.

Ogata [1958] has also carried out a numerical solution to equation 16, using a finite difference scheme similar to the one used here. He assumes that the parameter $\Delta\tau/\rho(\Delta\rho)^2$ or $\Delta\tau/k(\Delta\rho)^2$ (see equation 17) and $\Delta\rho$ are constant. Thus, as his solution progresses to larger and larger ρ values, $\Delta\tau$ must increase; however, he apparently assumes that $\Delta\tau$ is a constant, and so his numerical solution is in error. A check of his numerical calculations showed that they lagged the experimental results of this study and the results of *Lau et al.* [1959] by 50–100% in time at any radius.

In addition to the numerical solution of equation 15, several other analytical approaches were investigated; however, only one of these approaches gave a solution that agreed with the experimental findings. This method, used also by *Raimondi et al.* [1959], assumes that at some distance from the source, the influences of dispersion and diffusion on the concentration distribution, as the substance moves by a point, are small in comparison to the total dispersion and diffusion that has taken place up to that point. Thus, neglecting the right side of equation 15, we have that

$$\partial/\partial r \cong -(r/A)\,\partial/\partial t \qquad (22)$$

Introducing equation 22 into the dispersion and diffusion terms of equation 15 changes the spatial gradients to temporal gradients and leads to the expression

$$\frac{\partial c}{\partial t} + \frac{A}{r}\frac{\partial c}{\partial r} = \left[\alpha_1' \frac{r}{A} + D_m \frac{r^2}{A^2}\right]\frac{\partial^2 c}{\partial t^2} \qquad (23)$$

For the continuous injection of a substance at a steady rate with a concentration c_0 at $r = 0$, the solution to equation 23 is given by

$$c/c_0 = \tfrac{1}{2}\,\mathrm{erf_c}\left[\left(\frac{r^2}{2} - At\right)\Big/\left(\tfrac{4}{3}\alpha_1' r^3 + \frac{D_m}{A} r^4\right)^{1/2}\right] \qquad (24)$$

where $\mathrm{erf_c}\,[\Delta]$ is the complementary error function. Equation 24 was obtained by integrating with respect to time

$$c = (M/\bar{\rho}Q)(1/\sqrt{4\pi b})e^{-((a-t)/\sqrt{4b})^2} \qquad (25)$$

in which M is the mass of substance injected, $\bar{\rho}$ is density of fluid, Q is well flow rate, $a = r^2/2A$, and $b = (\alpha r^3/3A^2 + D_m r^4/4A^3)$. Equation 25 is the solution to equation 23 for an instantaneous injection of a mass of substance M at $r = 0$ and $t = 0$.

Equation 24 satisfies the boundary conditions (i.e., $\rho Q c_0$ = rate of mass supply at $r = 0$ and $c(r = \infty,\ t > 0) = 0$); however, it does not satisfy the initial condition, $c(r,\ t = 0) = 0$. In obtaining equation 24, $\partial c/\partial t$ was set equal to zero at $t = 0$. This assumption is approximately true away from the immediate vicinity of the source; however, it is not true within 10–20 particle diameters of the source. As a result of assuming $\partial c/\partial t = 0$ at $t = 0$, the approximate solution, equation 24, predicts a finite amount of mass in the media at $t = 0$. It should also be noted that equation 24 is the solution to equation 23 for the case where a constant concentration c_0 of tracer substance is maintained at the recharge well (i.e., $c(r = 0,\ t > 0) = c_0$).

Expressing equation 24 in the dimensionless form

$$\frac{c}{c_0} = \tfrac{1}{2}\,\mathrm{erf_c}\left[\frac{\rho^2/2 - \tau}{(4\rho^3/3)^{1/2}}\right] \qquad (26)$$

where D_m has been set equal to zero, $\rho = r/\alpha_1'$, and $\tau = At/\alpha_1'^2$, it has been plotted in Figures 3 and 4 for comparison with the numerical solutions. From these figures, it can be seen that the approximate solution, equation 26, at any τ predicts that the substance has moved farther into the media than is predicted from the numerical solution. The difference in area between these two solutions is a constant for all τ and is equal to the amount of mass, predicted by the approximate solution, that is present in the media at $\tau = 0$. The shape and standard deviation of concentration of the approximate and numerical solutions are, however, the same for all τ values. Thus, as τ increases, the approximate solution, equation 24, will give a good approximation of the concentration distri-

bution (for $\tau > 1000$ the time error between the approximate and numerical solutions is less than 1%).

Lau et al. [1959] suggested an approximate method by which the standard deviation of the concentration distribution may be estimated, based on the assumption that the concentration distribution is the linear sum of two effects: one due to longitudinal dispersion and the other due to the divergence of the streamlines. This assumption leads to the expression

$$\sigma = \sqrt{\tfrac{2}{3}\alpha_1(r - r_w^3/r^2)} \qquad (27)$$

where σ is the standard deviation for the concentration distribution, α_1 is the longitudinal dispersivity coefficient for uniform flow, and r_w is the radius of the well. For the case $r_w = 0$, the standard deviation obtained from the approximate solution (26) and that obtained from equation 27 have the same value

$$\sigma = \sqrt{(2/3)\alpha_1 r} \qquad (28)$$

provided that the dispersivity coefficient, α_1', along the radial streamlines is equal to α_1, the longitudinal dispersivity coefficient for uniform flow.

Experimental Equipment and Procedure

Equipment. To investigate the validity of the numerical and approximate solutions to equation 16 and to determine α_1', the dispersivity coefficient along the radial streamlines, a sand model was built and tested. A plan view of the model is shown in Figure 5. The model represented a horizontal confined aquifer with a fully penetrating well along one boundary and a perforated screen around the outer circular boundary. The circular boundary and open channel around the model enabled a constant head to be maintained on this boundary during the tests.

In the experiments a New Jersey Beach sand, having a mean diameter (d_{50}) of 0.167 cm and a uniformity coefficient (d_{60}/d_{10}) of 1.35, was used for the porous medium. The sand was confined between a plywood base and a lucite cover. Sheets of polyurethane sponge, placed on the plywood base and glued to the lucite cover, prevented the fluid from short circuiting along the top or bottom boundaries of the model, and, when compressed by the lucite cover, they gave a uniform and dense packing of the particles between the two boundaries.

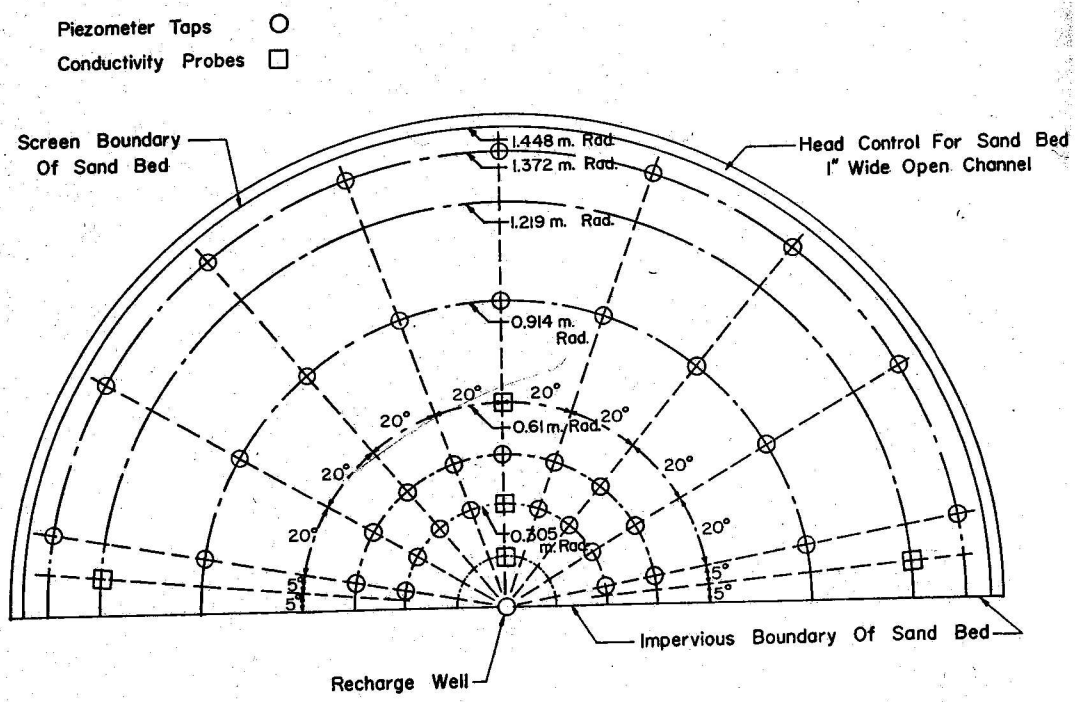

Fig. 5. Plan view of well recharge apparatus.

The thickness and porosity of the sand layer were 8.90 cm and 0.374, respectively.

The well was made from a 2.54-cm OD brass pipe with a fine mesh brass screen soldered to the pipe over ½ its circumference. A lucite manifold, extending the full depth of the well, rapidly distributed the fluid entering the well uniformly over its full length. The well was packed with the same media as in the model in order to reduce the volume of dead space above and below the model and to reduce any influence of differences between the mixing characteristics inside and outside the well on the measured concentration distributions.

In the experiments, a dilute solution of NaCl was used as a tracer since its presence could be detected by conductivity probes located within the well and at several points in the aquifer. The conductivity probes consisted of two parallel platinum plate electrodes, mounted at one end of a 0.64-cm, OD lucite tube [*Hoopes and Harleman,* 1965]. The maximum concentration of NaCl used was 0.1% in order to minimize density and viscosity differences between the fresh water and the tracer. The probes were calibrated against solutions of known concentrations of NaCl, and their response (deflection of the recording pen) was found to vary linearly with NaCl concentration for a tenfold change in concentration. The continuous injection of tracer at the well was accomplished by feeding both the salt water tracer and the fresh water to the recharge well through a three-way valve. In this way, a steady flow of fresh water could be rapidly changed to a steady flow of tracer at the same rate, or vice versa.

Piezometer taps, shown in Figure 5, were used to measure variations in the piezometric head.

Procedure. Before beginning a dispersion test, a steady-state flow pattern of fresh water was established throughout the model with a constant head in the outer channel. The rate of flow and the piezometric head distribution were measured; the radial variation of piezometric head was plotted on semilog graph paper and checked against equation 13. Having determined the head distribution, the conductivity probes in the recharging well and at locations 15.24, 30.48, and 60.96 cm into the media from the recharge well were balanced to read zero deflection on the Sanborn recorder. With the probes balanced, the 3-way valve was quickly changed to stop the fresh water flow and to start the salt water flow. When the tracer front had moved beyond the probe at a radius of 60.96 cm, the tracer measurements were completed; however, the salt water flow was maintained. The conductivity probes were rebalanced to read zero deflection in the salt water flow, and another run was begun, following the same procedure as before; in this case, however, fresh water displaced salt water. Experiments were performed at different flow rates, but, in all cases, the flow rate was adjusted so that the Reynolds number at the edge of the well was less than 6. This limit was placed on the flow rate in order that Darcy's law would apply throughout the model.

Data Analysis

To determine the dispersivity coefficient α_1' from the experimental measurements, the approximate solution, equation 24, was used. The use of the approximate solution to analyze the experimental results is discussed in the next section. If we define new variables $\xi = 2At_*/r^2$ and $\eta = (8/3)\alpha_1'/r$ where $t_* = t - t_{50,r}$ and if we set $D_m = 0$, then equation 24 becomes

$$c/c_0 = \tfrac{1}{2}\,\mathrm{erf_c}\,[(1 - \xi)/\sqrt{2\eta}] \qquad (29)$$

(Note that $A = Q/\pi b\theta$, since the flow field in the model has a width of 180°.) The correction $t_{50,r}$ was the time at which $c/c_0 = ½$ in the recharge well and accounted for the travel time between the three-way valve and the well. This correction was always less than 2% of the travel time to the probe 6 inches from the recharge well.

For any radial position, η is a constant, and, since the $\mathrm{erf_c}$ (Δ) is the integral of the Gaussian probability distribution, a plot of c/c_0 versus $1 - \xi$ on arithmetic probability paper results in a straight line with a standard deviation equal to $(\eta)^{1/2}$. Thus, knowing η, α_1' is given by

$$\alpha_1' = \tfrac{3}{8}r\eta = \tfrac{3}{8}r\sigma^2 \qquad (30)$$

where $\sigma = (\eta)^{1/2}$ is the standard deviation, determined from the plot of c/c_0 versus $1 - \xi$. The quantity $A = Q/\pi b\theta$ can be determined either from the tracer distribution at any radius (when $c/c_0 = \frac{1}{2}$ in equation 29, $A = r^2/2t_{50,r}$) or

from the rate of flow Q, the aquifer thickness, and the porosity. The permeability of the packing was determined using equation 13 (with the 2π changed to π) and the measurements of the radial piezometric head gradient.

A typical radial dispersion test (run 3) and its analysis are presented below to illustrate the method of data reduction. Figure 6 shows a plot of c/c_0 versus time of the experimental results and the approximate solution, equation 24, at the positions 15.24, 30.48, and 60.96 cm into the media from the recharging well. In Figure 7, c/c_0 is plotted against $1 - \xi$ on arithmetic probability paper. The lines of best fit through the data in Figure 7 give α_1' values of 0.16, 0.15, and 0.15 cm at 15.24, 30.48, and 60.69 cm, respectively, from the recharging well, using equation 30. The Reynolds number ($\mathfrak{R} = qd_{50}/\nu$ with $q = A/r$) at each of the three positions was 0.47, 0.23, and 0.12, respectively; the Reynolds number at the well was 5.6.

Presentation and Discussion of Results

Table 1 summarizes the radial dispersivity coefficients α_1' obtained from the experimental investigation along with the flow rates and the properties of the media used in the tests. For the Reynolds number range of this study, the experimental results indicate that α_1' has a constant value of 0.15 cm independent of the distance from the recharging well and the well flow rate. This value of α_1' agrees very well with α_1 obtained from longitudinal dispersion testing. If an equation, $D_1/\nu = \psi_1 (qd_{50}/\nu)$, is fitted at a Reynolds number of 1 to the results of *Harleman et al.* [1963] for longitudinal dispersion in sands ($n_1 = 1$ since it was assumed that the dispersion coefficient varies linearly with the seepage velocity), it is found that

$$D_1 = 0.86 d_{50} q = \alpha_1 q \qquad (31)$$

$$\alpha_1 = 0.86 d_{50} \qquad (32)$$

D_1 is the longitudinal dispersion coefficient and α_1 is the longitudinal dispersivity coefficient for uniform flow. Using the d_{50} of 0.167 cm for this sand gives $\alpha_1 = 0.14$ cm. From the laboratory tests in radial flow, $\alpha_1' = 0.15$ cm; thus, it is apparent that the dispersion coefficient ($D_1 = \alpha_1 q$ or $D_1' = \alpha_1' q$) along a streamline is the same for both uniform and nonuniform flows at the same velocity. Hence, experimental results for the longitudinal dispersion coefficient obtained for uniform flow, can be applied to

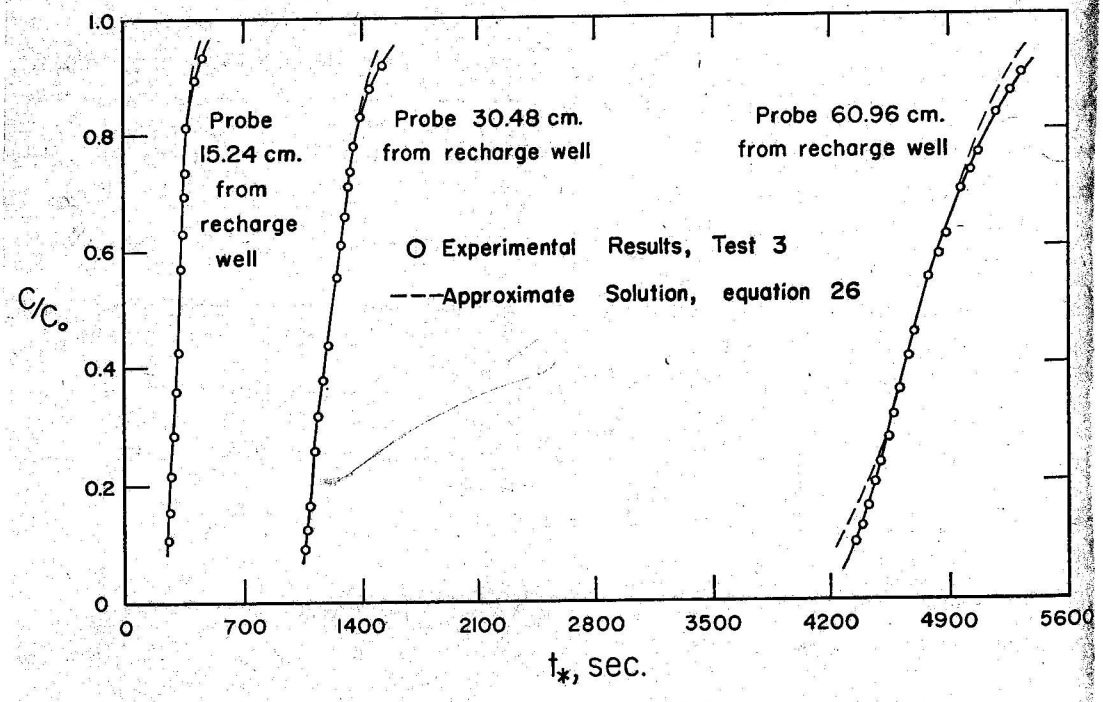

Fig. 6. c/c_0 versus t_* for three radii, radial dispersion test 3.

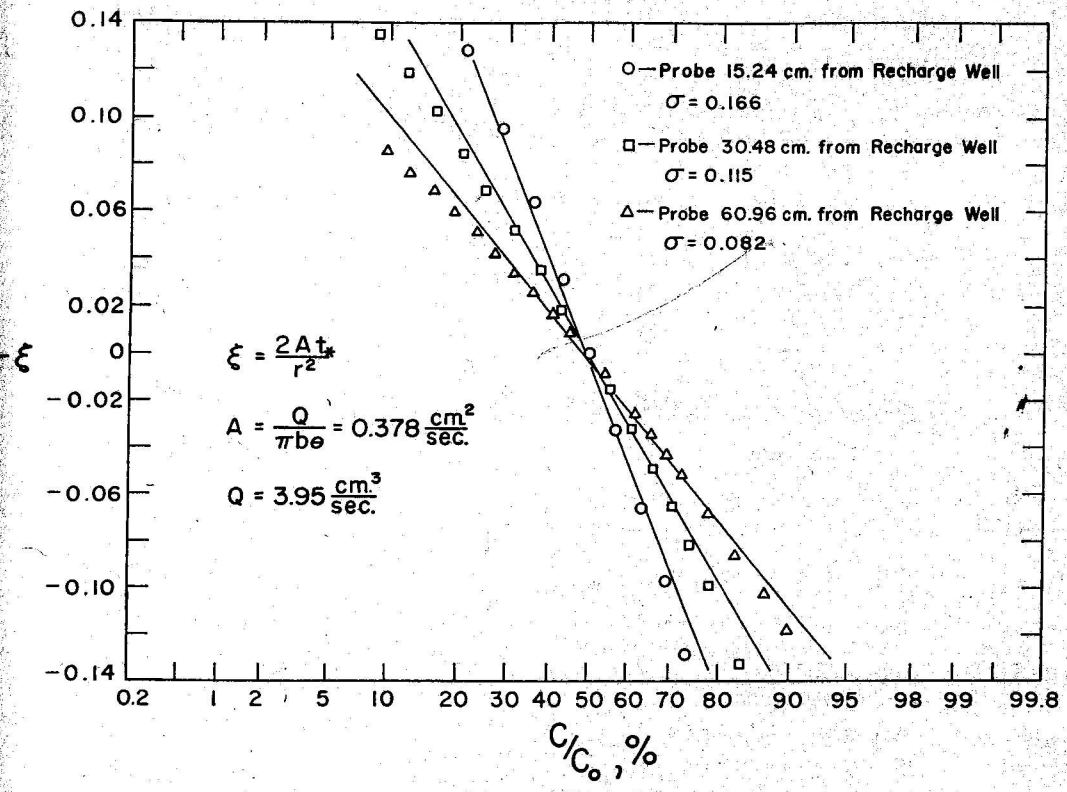

Fig. 7. c/c_0 versus $1 - \xi$, radial dispersion test 3.

dispersion problems involving nonuniform flows. As the media are isotropic and homogeneous, α_1' should be equal to α_1; however, little experimental confirmation of this fact has been previously reported.

Lau et al. [1959] in their experimental work found that α_1 and α_1' were equal at 22.86 and 45.72 cm from the well; however, at 91.44 cm from the well, α_1' was about 35% less than α_1 (perhaps owing to sampling errors). *Harpaz*

Table 1. Summary of Radial Dispersion Tests

Test	Radial Position from Recharge Well, cm	Q, cm³/sec	$R = \frac{qd_{50}}{\nu}$	α_1', cm	Remarks
1	15.24	2.82	0.34	0.15	No. 2 sand: d_{50} = 0.167 cm,
	30.48		0.17	0.15	UC = 1.35 = d_{60}/d_{10}
	60.96		0.09	0.15	
2	15.24	2.72	0.33	0.16	
3	15.24	3.82	0.47	0.16	θ = 0.374; K = 1.87 cm/sec
	30.48		0.24	0.15	
	60.96		0.12	0.15	
4	15.24	3.72	0.45	0.16	
5	15.24	1.98	0.24	0.15	$D_m = 0.95 \times 10^{-5}$ cm²/sec
	30.48		0.12	0.14	
	60.96		0.06	0.15	
6	15.24	1.90	0.23	0.15	

and Bear [1964] have presented laboratory and field measurements of tracer distributions in radial flow; however, values of α_1' were not given and their results could not be analyzed by equation 24, since they used different boundary and flow conditions.

In the analysis of the experimental results, the approximate solution, equation 24 with $D_m = 0$, to the radial flow dispersion was used, since the assumptions underlying its development (i.e., the tracer measurement points were located far enough from the recharge well so that $\partial/\partial r \cong -(r/A)\,\partial/\partial t$, equation 22, and $\partial c/\partial t \simeq 0$ at $t = 0$) were satisfied. As the probes were located at $\rho = 101.5$, 203, and 406, the approximate and numerical solutions of equation 16 at these positions are in close agreement (see Figures 3 and 4). In addition, the agreement in Figure 6 between the experimental results and the approximate solution also shows that the approximate solution, equation 24, does describe the concentration distribution in radial flow from a recharge well.

For run 5, with the minimum flow rate, at the probes 15.24, 30.48, and 60.96 cm from the recharge well, the numerical solution lags in time the approximate solution by about 1, 0.25, and 0.06%, respectively, of the mean travel time to each probe; thus, any time errors introduced by the use of the approximate solution will be very small. Molecular diffusion also had a negligible influence on the measured tracer distribution. The relative importance of molecular diffusion to radial dispersion can be obtained by taking the ratio of the two terms in the denominator of equation 24. Letting μ be this ratio gives

$$\mu = \frac{D_m r^4/A}{4/3\alpha_1' r^3} = \frac{3}{4}\frac{D_m r}{\alpha_1' A} \qquad (33)$$

For run 5 at the probe 60.96 cm from the recharge well, $\mu = 0.015$.

The volume of the dispersed region in the radial displacement process, as compared with the volume of fluid recharged, can be estimated from the standard deviation of the tracer distribution at any radius. Using $\pm 2\sigma$ of the mean radius r as a measure of the width of the dispersed zone (includes 95% of the dispersed region), the ratio of the volume of the dispersed region to the volume of the fluid recharged is given by

$$\frac{4\sigma}{r} = \left(\frac{32}{3}\frac{\alpha_1'}{r} + \frac{8D_m}{A}\right)^{1/2} \qquad (34)$$

For the conditions of run 5 at the probe farthest from the recharge well (i.e., $r = 60.96$ cm), $4\sigma/r = 0.16$, or the volume of the dispersed region is 16% of the total recharged volume.

Though the theoretical predictions developed in this investigation have been applied to the study of radial dispersion in a small sand model, these results may also be applied to field situations. As an example, consider a confined aquifer, 30.5 meters thick, composed of a fine sand ($d_{\infty} = 0.305$ mm) which contains small amounts of gravel and silt. The aquifer has a porosity of 0.35 and a permeability of 0.047 cm/sec (these conditions are typical of the confined aquifer at Manhattan Beach in Los Angeles, California). For a 30.5-cm-diameter well, fully penetrating and steadily recharging the aquifer with treated waste water at a rate of 0.018 m³/sec, the quantity $A = Q/2\pi b\theta = 2.70$ cm²/sec. The flow in the aquifer will be laminar and α_1' is 0.026 cm (α_1' may be determined from equation 32).

The relative influence of molecular diffusion to radial dispersion on the distribution of recharged water in the mixed region between the recharged water and the native groundwater is given by μ in equation 33; assuming $D_m = 1.0 \times 10^{-5}$ cm²/sec, $\mu = 0.35$ at 30.5 meters from the well and 3.5 at 305 meters from the well. Thus, close to the well, dispersion governs the mixing, whereas at large distances from the well, the mixed region is governed by molecular diffusion. The extent of the mixed or dispersed region during recharging can be estimated from $4\sigma/r$ in equation 34. For a point 30.5 meters from the well, $4\sigma/r$ is equal to 0.011, and, at 305 meters from the well, $4\sigma/r$ is equal to 0.006. Thus, the zone of mixing of the recharged water with the native groundwater for this recharging well is confined to a 0.3-meter region at a radius of 30.5 meters from the well and a 1.8-meter region at a radius of 305 meters from the well.

Summary and Conclusions

This investigation has dealt with miscible fluid displacement problems occurring in the recharge and disposal of treated and untreated water by a single well in a groundwater basin.

The mass conservation equation for a dissolved substance in a two-dimensional groundwater flow was developed. For the idealized conditions of a homogeneous isotropic confined aquifer, analytical predictions of the radial and temporal distribution of a tracer during recharging by a single well have been made and compared with experimental measurements of the tracer distribution. In addition, the analytical solutions have been used to study the relative influences of convection, dispersion, and molecular diffusion on the tracer distribution.

The distribution of a dissolved substance in steady radial flow from a well is given by the approximate solution, equation 24. Neglecting molecular diffusion, a comparison of equation 24 with a numerical solution of the differential equation describing the tracer distribution (see Figures 3 and 4) indicated that equation 24 is a close approximation of the tracer distribution for distances greater than 20 particle diameters from the well. The influence of molecular diffusion on the tracer distribution was not important in the experimental study; however, in field operations at distances of only 91.4 meters from the well, molecular diffusion may be of equal importance with radial dispersion in determining the tracer distribution. The example application of these results to a field situation indicated that the dispersed or mixed region is small in comparison to the total volume of fluid recharged. Finally, the results of the experimental study showed that the dispersion coefficient along the streamlines in radial flow is equal to the coefficient of longitudinal dispersion in uniform flow at the same velocity; thus, measurements of dispersion coefficients in uniform flow may be used in the study of dispersion and displacement problems in nonuniform flow.

Acknowledgments. The authors would like to express their appreciation to Mr. Khalid Mohtadullah for his assistance in the experimental work. This work was carried out at the Hydrodynamics Laboratory of the Massachusetts Institute of Technology and constituted one phase of a research project, sponsored by the Division of Water Supply and Pollution Control, Public Health Service, National Institutes of Health, U. S. Department of Health, Education, and Welfare under research grant WP-347. The IBM 7094 computer in the Computation Center at the Massachusetts Institute of Technology was used to carry out the numerical solutions of this investigation.

References

Bachmat, Y., and J. Bear, The general equations of hydrodynamic dispersion in homogeneous, isotropic, porous mediums, *J. Geophys. Res., 69*(12), 2561–2567, 1964.

Bear, J., On the tensor form of dispersion in porous media, *J. Geophys. Res., 66*(4), 1185–1197, 1961.

Harleman, D. R. F., P. F. Mehlhorn, and R. R. Rumer, Jr., Dispersion-permeability correlation in porous media, *J. Hydraulics Div. Am. Soc. Civil Engrs., HY2*, 67–85, March 1963.

Harleman, D. R. F., and R. R. Rumer, Jr., The dynamics of salt-water intrusion in porous media, *Massachusetts Inst. Technol. Dept. Civil Engr., Hydrodynamics Lab., Rept. 55*, August 1962.

Harpaz, Y., and J. Bear, Investigations on mixing of waters in underground storage operations, *Assoc. Sci. Hydrol., Intern. Union Geod. Geophys., Publ. 64* (13th General Assembly, Berkeley, Calif.), 132–153, 1964.

Hoopes, J. A., and D. R. F. Harleman, Waste water recharge and dispersion in porous media, *Massachusetts Inst. Technol. Dept. Civil Engr., Hydrodynamics Lab., Rept. 75*, June 1965.

Kitagawa, K., Sur le dispersement et l'écart moyen de l'écoulement des eaux sout erranines: l'expériences avec un modèle de laboratoire, *Mem. Coll. Sci., Univ. Kyoto, Ser. A, 17*, 37–42, 1934.

Lau, L. K., W. J. Kaufman, and D. K. Todd, Studies of dispersion in a radial flow system, *Univ. Calif. Sanit. Engr. Res. Lab., Progr. Rept. 3*, July 1957.

Lau, L. K., W. J. Kaufman, and D. K. Todd, Dispersion of a water tracer in radial, laminar flow through homogeneous porous media, *Univ. Calif. Hydrol. Sanit. Engr. Res. Lab., Progr. Rept. 5*, July 1959.

Ogata, A., Dispersion in porous media, Ph.D. dissertation, Northwestern University, Evanston, Ill., 1958.

Raimondi, P., G. H. G. Gradner, and C. B. Petrick, Effect of pore structure and molecular diffusion on the mixing of miscible liquids flowing in porous media, *American Institution of Chemical Engineers-Society of Petroleum Engineers Conference*, Preprint 43, December 1959.

Richtmyer, R. D., Difference methods for initial-value problems, tract 4, *Interscience Tracts in Pure and Applied Mathematics*, 238 pp., Interscience, New York, 1962.

Rumer, R. R., Jr., Longitudinal dispersion in steady and unsteady flow, *J. Hydraulics Div., Am. Soc. Civil Engrs., HY4*, 147–172, July 1962.

Sanitary Engineering Research Laboratory, University of California, Studies in water reclamation, *Tech. Bull. 13*, July 1955.

Scheidegger, A. D., General theory of dispersion in porous media, *J. Geophys. Res., 66*(10), 3273–3278, 1961.

(Received November 17, 1966.)